

Highly efficient top-emitting white organic light-emitting diodes with improved contrast and reduced angular dependence for active matrix displays

Guohua Xie, Zhensong Zhang, Qin Xue, Shiming Zhang, Li Zhao, Yang Luo, Ping Chen, Baofu Quan, Yi Zhao^{*}, Shiyong Liu^{*}

State Key Laboratory on Integrated Optoelectronics, College of Electronic Science and Engineering, Jilin University, 2699 Qianjin Street, Changchun 130012, PR China

ARTICLE INFO

Article history:

Received 6 July 2010

Received in revised form 30 September 2010

Accepted 2 October 2010

Available online 14 October 2010

Keywords:

Top-emitting

White light

Cu

Capping layer

ABSTRACT

Highly efficient top-emitting white organic light-emitting diodes (TEWOLEDs) on silicon substrates based on complementary blue and yellow phosphors are demonstrated. The bottom copper anode with medium reflectance, which is compatible with standard complementary metal oxide semiconductor (CMOS) technology, and the semitransparent cathode with a top capping layer, are introduced to facilitate white light emission with improved contrast and reduced angular dependence. Both TEWOLEDs, with and without the capping layers, exhibit nearly lambertian-type emission. The spectrum of TEWOLED with a capping layer is similar to that of the bottom-emitting counterpart. Our TEWOLED reaches high efficiencies of 27.7 cd/A and 17.6 lm/W at a current density of 10 mA/cm², and low voltage of 4.4 V at 1000 cd/m².

© 2010 Elsevier B.V. All rights reserved.

1. Introduction

Organic light-emitting diodes (OLEDs) are considered as one of the most powerful candidates for the next generation mainstream flat panel displays and solid-state lighting sources [1–5]. In active matrix displays, top-emitting architectures are preferable due to their intrinsic large aperture ratio and the less risk of cross-talk in high resolution and large area displays. For full color and high resolution displays, white light combined with color filters is one of the best schemes for low-cost mass production due to the avoidance of precise and time-consuming shadow mask process for red-green-blue (RGB) pixilation [6,7]. It's pointed out that the technique which is capable of directly patterning the pixels in small dimensions (~10 μm pitch for RGB pixels) is not available so far [8]. Note that the pixel pitch of OLED microdisplays now is reduced to

several micrometers to achieve high resolution. However, it's a great challenge to achieve uniform and angular independent white light emission in the top-emitting architectures due to intrinsic strong microcavity effects. Basically, a low reflective bottom anode and a highly transparent top cathode stack are beneficial for white light extraction from top-emitting architectures avoiding constructive interference inside the devices [3,9–17]. In order to achieve high resolution and high information-content Si-based microdisplays, which have vast potential application in military and consumer electronics market, TEWOLED is one of the prerequisites as well as CMOS process selection. As mentioned above, no technique is competent enough to directly pattern the full color OLED pixels in microdisplays. The solution now is based on white light and RGB color filters. For low cost mass production, a suitable active matrix driving circuit scheme introducing the standard CMOS metal interconnection (Al or Cu) is crucial, as it has to meet the requirement of fabricating OLEDs directly on the top metal layer of the chips. In addition, TEWOLEDs based on Cu foil with high flexibility are very promising for flexible full color active matrix displays.

^{*} Corresponding authors. Tel.: +86 431 85168242-8301.

E-mail addresses: zhao_yi@jlu.edu.cn (Y. Zhao), syliu@jlu.edu.cn (S. Liu).

In this letter, we demonstrate highly efficient TEWOLEDs based on Cu bottom anode, which is compatible with the standard foundry CMOS technology (for deep submicron and below), paving the way for integrating organic optoelectronic devices directly with the readily available Si wafer. It's reported that the production cost comes from the interconnect metallization process in integrated circuits is over 50% of the total budget [18]. A new choice of metal process, which is not compatible with the standard foundry technology, will cost even much more. Undoubtedly, this is a great obstacle for mass production. In previously reported TEWOLEDs, Ag [11,16], Ag/ITO [14], Al [17], Al/Ag [17], Al/Au [13], Al/ITO [19], Al/Ni [10], and Mo [15] are selected as anodes, respectively. However, only limited candidates are competent for commercialization. Here, a Cu anode is adopted for TEWOLED to meet the requirement of integrating OLEDs with foundry CMOS circuitry. Cu can then be used as contact material and as via connection in the CMOS process [18,20]. In contrast, an Al interconnect requires a W plug for via and subsequently creates an additional interface of Al and W. No such interface is existing between the via and interconnect for Cu as via and anode material for OLEDs. This does significantly simplify the fabricating process for OLED microdisplays aiming for low cost and small size with augmented reality that requires high resolution [4]. In addition, due to the excellent thermal conductivity, Cu-based devices usually exhibit superior heat dissipation [21], thus the issue of thermal management in highly dense integrated devices tends to be less severe. In order to further reduce the OLED microcavity effect, an additional capping layer, 4,4',4''-tris(N-3-methylphenyl-N-phenyl-amino)triphenylamine (m-MTDATA), is deposited directly over the semitransparent cathode. It's proved here that the manipulation of white light emission profiles towards angular independence and broad spectral coverage is much easier in Cu-based TEWOLEDs than those based on highly reflective electrodes, such as Ag and Al.

2. Experimental

The white OLED is based on the blue emitter iridium(III) bis[(4,6-difluorophenyl)pyridinato-N,C^{2'}] (Flrpic) and the yellow emitter bis(2-(2-fluorophenyl)-1,3-benzothiazolone-N,C^{2'}) ((F-BT)₂Ir(acac)) doped into a common host, N, N'-dicarbazolyl-3,5-benzene (mCP), respectively. Pristine m-MTDATA, N,N'-bis(naphthalene-1-yl)-N, N'-bis(phenyl)benzidine (NPB), and 7-diphenyl-1,10-phenanthroline (BPhen) serve as hole injecting layer, hole transporting layer, and hole blocking/electron transporting layer, respectively. The Cu anode is thermally deposited onto Si substrate covered with insulating SiO₂, following with m-MTDATA:MoO_x p-doping layer to reduce the ohmic loss. The structures are listed below, Si/SiO₂/Cu (60 nm)/m-MTDATA:MoO_x (15wt.%, 10 nm)/m-MTDATA (18 nm)/NPB (5 nm)/mCP (15 nm)/mCP:Flrpic (10wt.%, 5 nm)/BPhen (2 nm)/mCP:(F-BT)₂Ir(acac) (4wt.%, 5 nm)/BPhen (40 nm)/LiF (1 nm)/Al (2 nm)/Ag (18 nm)/m-MTDATA (0 and 50 nm). For comparison, ITO/m-MTDATA:MoO_x(15wt.%, 10 nm)/m-MTDATA (18 nm)/NPB (5 nm)/mCP (15 nm)/

mCP:Flrpic (10wt.%, 5 nm)/BPhen (2 nm)/mCP:(F-BT)₂Ir(acac) (4 wt.%, 5 nm)/BPhen (40 nm)/LiF (1 nm)/Al (100 nm), a bottom-emitting white OLED (BEWOLED) is also fabricated. In order to achieve high efficiency, the pristine 15 nm mCP is introduced to prevent the high energy triplet exciton of blue emitter from diffusing into the NPB layer, and 2 nm BPhen spacer is inserted between the blue and yellow emitters to balance white emission. The current-voltage-luminance characteristics were measured with a PR650 spectrascan spectrometer and a Keithley 2400 programmable voltage-current source. All the devices without encapsulation were measured in ambient atmosphere at room temperature.

It's reported that the out-coupling characteristics are significantly dependent on the interference effects in the cavity [22,23]. As depicted, the top light out-coupling stack design strongly influences the emission profiles [9–11,13–17,19,23,24]. In order to reveal the effects, we investigate the influences of the capping layer on the reflectance, transmittance and absorbance of the stack of BPhen/LiF/Al/Ag/m-MTDATA (x nm) with software SETFOS [25].

3. Results and discussion

For monochromatic emission, the out-coupling efficiency is not simply dependent on the transparency of the top electrode [23]. It's even more complicated in TEWOLEDs, because of the complex interplay of wide-angle and multiple-beam interference effects. As indicated in Fig. 1a and b, the stack with 50 nm capping layer exhibits a low reflectance and high transmittance in the blue region, but medium values in the yellow region. Additionally, the stack with above 50 nm capping layer has low absorbance over the visible region (Fig. 1c). However, the devices with a capping layer above 50 nm do not exhibit improved luminance (not shown here).

As shown in Fig. 2, TEWOLED with (Device A) and without (Device B) 50 nm capping layer exhibit similar luminance-voltage characteristics, while Device A has superior luminance due to the improved light out-coupling efficiency. In contrast, the luminance of BEWOLED (Device C) tends to grow more slowly as the voltage increased. One of the reasons may be attributed to the different series resistance of the electrodes. And also, the lower thermal conductivity of the ITO/glass substrate than that of Cu/SiO₂/Si substrate may play a role, as great joule heat generated on the poor thermal conductive substrate may accelerate the degradation at high luminance level. In view of practical use, the capping layer is not only beneficial for the improvement of luminance of TEWOLED, but also for the achievement of high contrast active matrix displays. Device A with the capping layer reaches a contrast ratio of 199, while that of Device B is only 66, under an ambient illumination of 140 lx [26,27]. A high contrast ratio is necessary to achieve high gray scale and reduce eyestrain in near-eye microdisplays with relative low perceptible luminance level. As for head-mount displays, the ambient illumination could be much lower. Taking 10 lx for example, the contrast ratio of Device A is up to 351 when the on-state brightness is set to 200 cd/m².

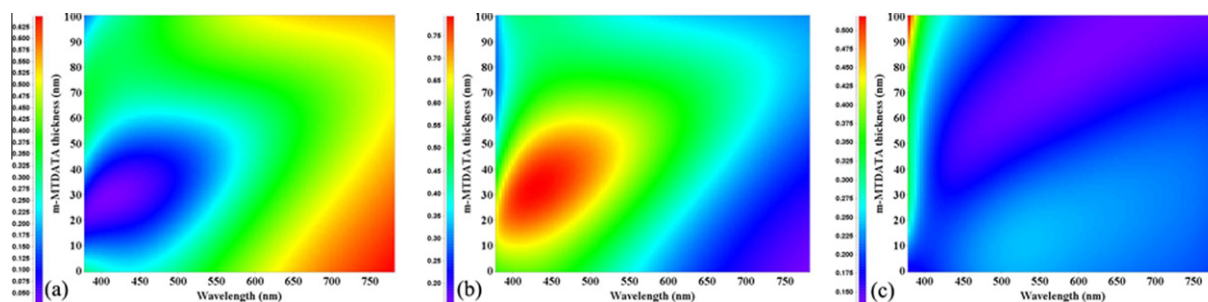


Fig. 1. (a–c) Calculated reflectance, transmittance and absorbance of the stack BPhen (40 nm)/LiF (1 nm)/Al (2 nm)/Ag (18 nm)/m-MTDATA (x nm) as a function of m-MTDATA capping layer thickness and the wavelength, respectively. The optical constants used in the calculation are obtained by variable-angle spectroscopic ellipsometry measurements. The dispersion of the complex refractive indices is also taken into account, as the emission profiles are dependent on the dispersion.

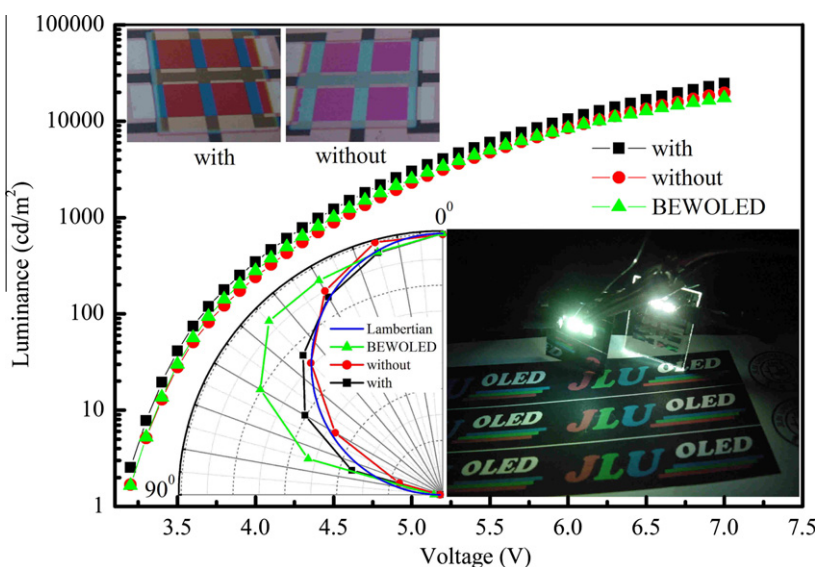


Fig. 2. Luminance–voltage characteristics of Device A, B and C, respectively. The lower left-hand inset indicates the measured angular distribution of the devices and the bluish solid line represents a Lambertian-type distribution. The upper left-hand inset shows the photos of TEWOLEDs with and without the capping layer, respectively. TEWOLED with the capping layer and BEWOLED radiate at a high brightness level are also presented in the lower right-hand inset.

The current efficiency–current density–power efficiency characteristics of the three devices are compared in Fig. 3. Apparently, TEWOLEDs exhibit lower efficiency at low luminance, while peak efficiency at low luminance is observed in BEWOLED, and subsequently the efficiency gradually decreases due to triplet–triplet annihilation as the current density increases [23]. At the current density of 10 mA/cm², the efficiencies are 27.7 cd/A (17.6 lm/W), 24.8 cd/A (15.4 lm/W) and 26.8 cd/A (16.5 lm/W) for Device A, B and C, respectively. As shown in the inset of Fig. 3, the spectra of TEWOLEDs are narrower in the red region due to interference effects and the poor transmittance of the cathode stack at long wavelengths, which have been indicated in Fig. 1. According to our calculation, the BEWOLED is not optimized with the structure used here. The optimized current efficiency is expected to be improved by 40%, simply adjusting the thicknesses of m-MTDATA:MoO_x and m-MTDATA layer to improve light out-coupling in BEWOLED. Hence the optimized BEWOLED

would still have slightly superior efficiencies. A thick p-doping layer with negligible voltage drop is also expected to improve the yield of both TEWOLEDs and BEWOLEDs in mass production.

With the capping layer, the angular dependence of the spectrum in TEWOLED is reduced, while the spectrum of TEWOLED without the capping layer changes dramatically as the viewing angle changes, shown in Fig. 4a and b. BEWOLED exhibits almost no angular dependence of the spectrum (Fig. 4c). The Commission Internationale de L'Eclairage (CIE) coordinates measured in forward direction of Device A only change from (0.306, 0.430) to (0.330, 0.445) over the luminance range of 100–4000 cd/m², and the variation is only (± 0.003 , ± 0.001) over 4000–20000 cd/m². Due to the dominant yellow emission as a result of constructive interference in Device B, the CIE coordinates are quite stable over 100–20000 cd/m², with negligible variation of (± 0.009 , ± 0.004). Device C (BEWOLED) has a convoluted shape of the CIE coordinates over

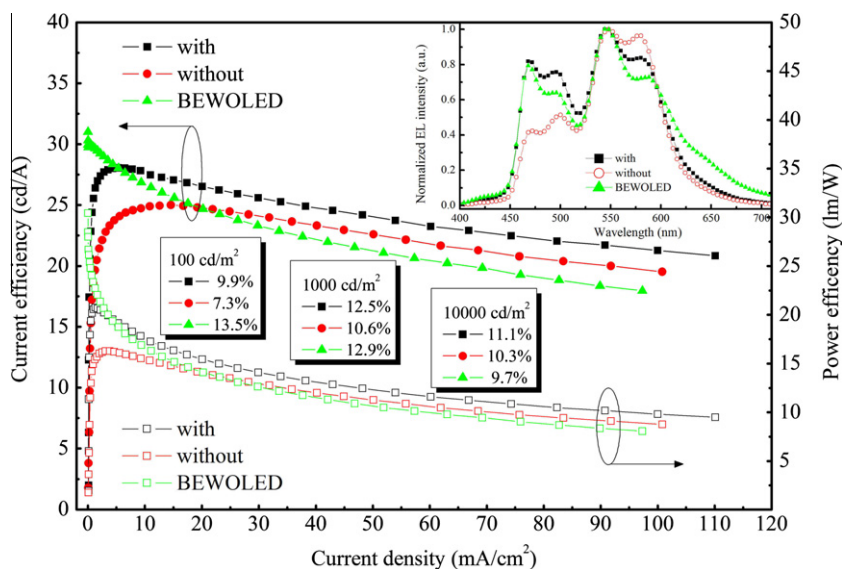


Fig. 3. Current efficiency–current density–power efficiency characteristics of Device A, B and C, respectively. The external quantum efficiencies at a luminance of 100, 1000, 10000 cd/m² are also shown in the boxes. Inset: the electroluminescent (EL) spectra of the devices at a current density of 40 mA/cm².

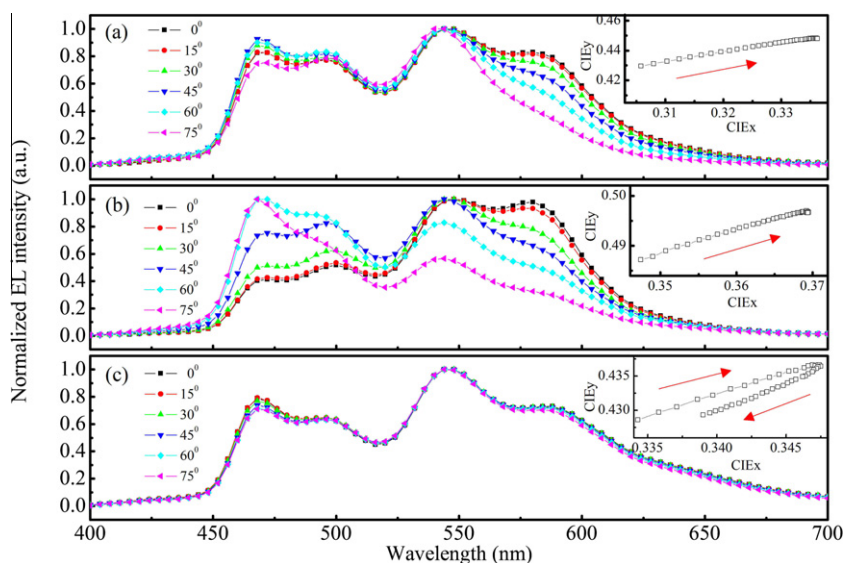


Fig. 4. Spectra of Device A, B and C at a current density of 40 mA/cm², respectively. CIE 1931 color coordinates measured in forward direction over a luminance range of 100–20,000 cd/m² are also plotted in the insets, respectively.

the luminance range, corresponding to a variation of (± 0.006 , ± 0.004). The blue-shift of the color in Device C may be caused by the slightly increased residual NPB emission under high driving voltage. However, this emission is suppressed in TEWOLEDs with an optical cavity length of ~ 100 nm as the low light out-coupling efficiency in the deep-blue region, which is also indicated by the whole device simulation with software SETFOS. That's why the variation of the CIE coordinates with luminance of TEWOLEDs is different to that of BEWOLED.

4. Conclusions

In summary, we have demonstrated efficient TEWOLED based on Cu anode for potentially full color small and large area active matrix displays, or flexible OLED displays. In this embodiment, we have deliberately considered the technologic compatibility of integrating OLEDs with CMOS circuitry, aiming for commercially low-cost OLED microdisplays. In order to improve the contrast ratio (typical for microdisplays), and reduce the angular dependence

(typical for flexible displays), a low absorption loss capping layer is used to balance the degree of constructive and destructive interference for white light extraction.

Acknowledgements

We wish to acknowledge funding for this research from the National Key Basic Research and Development Program of China under grant No. 2010CB327701, and the National Natural Science Foundation of China (grant Nos. 60977024 and 60907013). The authors gratefully acknowledge Dr. Liying Zhang and Dr. Bin Li for providing (F-BT)₂Ir(acac).

References

- [1] O. Prache, *Displays* 22 (2001) 49.
- [2] J.Y. Lee, J.H. Kwon, H.K. Chung, *Org. Electron.* 4 (2003) 143.
- [3] S. Kim, S. Lee, M. Kim, J. Song, E. Hwang, S. Tamura, S. Kang, H. Kim, C. Kim, J. Lee, J. Kim, S. Cho, J. Cho, M.C. Suh, H. Kim, *J. Soc. Inf. Disp.* 17 (2009) 145.
- [4] A.P. Ghosh, T.A. Ali, I. Khayrullin, F. Vazan, O.F. Prache, I. Wacyk, *Proc. SPIE* 7415 (2009) 74150Q.
- [5] S. Reineke, F. Lindner, G. Schwartz, N. Seidler, K. Walzer, B. Lüssem, K. Leo, *Nature* 459 (2009) 234.
- [6] K. Mameno, R. Nishikawa, K. Suzuki, S. Matsumoto, T. Yamaguchi, K. Yoneka, Y. Hamada, H. Kanno, Y. Nishio, H. Matsuoka, Y. Saito, S. Oima, N. Mori, G. Rajeswaran, S. Mizukoshi, T.K. Hatwar, *Proc. IDW'02, The Ninth International Display Workshop, Hiroshima, Japan* (2002) 235.
- [7] W. den Boer, *Active Matrix Liquid Crystal Displays: Fundamentals and Applications*, Elsevier, Amsterdam, 2005.
- [8] D. Armitage, I. Underwood, S.-T. Wu, *Introduction to Microdisplays*, Wiley, New York, 2006. pp. 269.
- [9] T. Feng, T.A. Ali, E.S. Ramakrishnan, R. Campos, W.E. Howard, *Proc. SPIE* 4105 (2001) 30.
- [10] H. Kanno, Y. Sun, S.R. Forrest, *Appl. Phys. Lett.* 86 (2005) 263502.
- [11] S.-F. Hsu, C.-C. Lee, S.-W. Hwang, C.H. Chen, *Appl. Phys. Lett.* 86 (2005) 253508.
- [12] J.P. Spindler, T.K. Hatwar, S.A. Van Slyke, *SID IDRC* (2006) 51.
- [13] X. Zhu, J. Sun, X. Yu, M. Wong, H.-S. Kwok, *Jpn. J. Appl. Phys.* 46 (2007) 4054.
- [14] M.S. Kim, C.H. Jeong, J.T. Lim, G.Y. Yeom, *Thin Solid Films* 516 (2008) 3590.
- [15] M.-T. Lee, M.-R. Tseng, *Curr. Appl. Phys.* 8 (2008) 616.
- [16] M. Thomschke, R. Nitsche, M. Furno, K. Leo, *Appl. Phys. Lett.* 94 (2009) 083303.
- [17] P. Freitag, S. Reineke, M. Furno, B. Lüssem, K. Leo, *Proc. SPIE* 7722 (2010) 77221D.
- [18] K.N. Tu, *J. Appl. Phys.* 94 (2003) 5451.
- [19] R.S. Cok, J.D. Shore, *J. Soc. Inf. Disp.* 17 (2009) 617.
- [20] R. Doering, Y. Nishi, *Handbook of Semiconductor Manufacturing Technology*, 2nd ed., Taylor & Francis, CRC, London, 2007.
- [21] Y.-S. Tsai, S.-H. Wang, C.-H. Chen, C.-L. Cheng, T.-C. Liao, *Appl. Phys. Lett.* 95 (2009) 233306.
- [22] H. Riel, S. Karg, T. Beierlein, B. Ruhstaller, W. Rieß, *Appl. Phys. Lett.* 82 (2003) 466.
- [23] Q. Huang, K. Walzer, M. Pfeiffer, V. Lyssenko, G. He, K. Leo, *Appl. Phys. Lett.* 88 (2006) 113515.
- [24] Q. Wang, Z. Deng, J. Chen, D. Ma, *Opt. Lett.* 35 (2010) 462.
- [25] www.fluxim.com
- [26] J.A. Dobrowolski, B.T. Sullivan, R.C. Bajcar, *Appl. Opt.* 31 (1992) 5988.
- [27] In the calculation, the brightness of the devices at off-and on-state is set to be 0 and 1000 cd/m². The standard illuminating source D65 is referenced as the spectral power distribution of the light source to determine the luminous reflectance taking into account the response of human eyes.